Basrah Journal for Engineering Sciences, Vol. 22, No. 2, (2022), 49-56

Original Article

Journal homepage: www.bjes.edu.iq
ISSN (Online): 23118385, ISSN (Print): 18146120

OPEN ACCESS

Effect of Defects Parameters of Welded Joints on Fatigue Life using Finite Element Analysis

Laila F. Abdullatif [1,*], Nathera A. Saleh [2]

[1,2] *Department of Mechanical Engineering, College of Engineering, University of Basrah, Basrah, Iraq*
E-mail addresses: lailafadhl3@gmail.com , nathera.saleh@uobasrah.edu.iq
Received: 24 April 2022; Revised: 26 May 2022; Accepted: 6 June 2022; Published: 24 December 2022

Abstract

The present investigation's main goal is to assess butt joint and T-joint plates containing misalignment, undercut and porosity welding defects by studying the influence of the defect's parameters on the fatigue life. The fatigue life is predicted using ANSYS ver. 19 Software. The results of finite element analysis are used in the regression analysis to find relationship between the fatigue life and defects parameters. The findings demonstrated that finite element modeling and the pervious published experimental tests were in good agreement with maximum error percentage 4 %. The fatigue life differed substantially depending on the defect's parameters.

Keywords: Finite element method, Fatigue life, Welding defects.

https://doi.org/10.33971/bjes.22.2.8

1. Introduction

The process of heating and cooling during welding has a significant impact on the material, as well as by the addition of filler material, resulting in inhomogeneous material zones. Because of this, welded structures develop flaws [1]. When the welded component is subjected to cyclic fatigue load, these flaws can have a considerable impact on the local stress field around the welds. As a result, fatigue assessments are very useful for all cyclically loaded welded structures, such as ships, offshore structures, cranes, bridges, vehicles, railcars, etc.

Mashiri et al. [2] determined the influence of weld profile and weld undercut on fatigue fracture propagation life when subjected to cyclic tensile loading by numerical analysis of non-load-bearing thin-walled cruciform joints in two dimensions. They found that the fatigue resistance of a concave weld profile is higher and when there is a bigger undercut depth, the fatigue performance suffers. Frostevarg et al. [3] studied the major reasons for the creation of several forms of undercuts in hybrid laser-arc welding of butt joint welds. They found that in Laser Beam Welding (LBW), three different undercut kinds for butt joint welds were observed, three in Gas Metal Arc Welding (GMAW) and there are six different forms of arc leading Laser Arc Hybrid Welding (LAHW). Steimbreger et al. [4] deal with a fracture mechanics technique that predicts the fatigue limit of welded components with undercuts using the Resistance Curve theory. The most impacting variable, according to the findings, is depth, which can be employed as a limiting element in design standards. Andrews [5] and Ottersbock et al. [6] investigated of axial misalignment on the load-carrying transverse cruciform welded joints' fatigue strength and specimen of butt-welded ultra-high-strength steel using fracture mechanics and experimental approaches. They found that misalignment considerably lowered the fatigue strength when failure occurred due to cracking from the weld toe. Surojo et al. [7] studied the fracture growth rate of underwater wet welded low carbon steel SS400 which is affected by water flow speed and water depth. Underwater wet welded joints exhibit more weld flaws, such as porosity, incomplete penetration, and irregular surface, than air welded joints. Results showed the higher the water flow rate, the more welding faults there are, which reduces fatigue crack resistance. Nguyen [8] studied the impacts of several influential weld geometry factors, residual stresses, and combined axial and bending loadings on the fatigue behavior of butt-welded steel joints by creating a mathematical model to predict the fatigue S-N curves and fatigue notch factor. The present study provides the basic understanding of the combined effect of weld geometry, residual stresses and the combined loadings on the fatigue behavior of butt-joints. Heshmati [9] investigated several frequently used bridge details using the nominal stress, structural hot spot stress and effective notch stress approaches. The goal of this study is to determine whether these approaches are equivalent in terms of the fatigue strength of the analyzed details. Various modeling strategies are used to carry out finite element modeling. The implementation of the structural hot spot tress approach in the field of bridge engineering appears to be more reasonable, based on the obtained results. Steimbreger [10] analyzed fatigue strength of transverse non-carrying load fillet joint. As-welded and enhanced joints were subjected to high-frequency axial fatigue tests. The weld toe was altered into more suitable designs using TIG-dressing and shot peening procedures. TIG dressing was found to provide smoother toes and extended fatigue life by at least 50 % and as-welded (AW) samples welded to requirements have greater fatigue strength than FAT 90. Saleh et al. [11] studied the influence of the flaws size on the failure pressure of an API 5L X52 pipe line with partial penetration,

undercut, and porosity welding flaws under internal pressure. The pressure is estimated using ANSYS ver.19 Software. According to the findings, the partial penetration flaw was the most serious flaw on the pipeline's failure pressure, while the undercut flaw was the least serious.

According to the studies described above, there are only a few researchers working on forecasting the fatigue life of butt joint and T-joint fillet welds with welding faults. As a result, a large number of models, comprising a wide range of welding flaw sizes of undercut, misalignment, and porosity flaws, have been modeled using finite element modeling in the current work. The findings were also used in a regression analysis to create a model that could forecast the fatigue life of the assessed flaws.

2. Finite element simulation

2.1. Material characteristics

Table 1 shows the mechanical characteristics of the modeled plates that were utilized in Finite Element Analysis and submitted for ANSYS Workbench Software in Engineering Data.

Table 1. Mechanical characteristics for the simulated plates of steel grade S355J2 + N.

Properties	Values	Units
Yield stress	375	MPa
MYS (minimum yield stress)	355	MPa
Ultimate tensile stress	550	MPa
Weld metal tensile strength	570	MPa
Weld metal yield strength	450	MPa
Heat affected zone tensile strength	500	MPa
Heat affected zone yield strength	355	MPa

2.2. Plate's geometries

The current project was carried out using numerical simulation models by ANSYS Workbench Software. The simulated plates were T-joint fillet weld & butt joint. Table 2 shows the dimensions of the simulated plates used in the present work. Figures 1 and 2 show the design of butt joint plate and T-joint fillet weld respectively.

Table 2. Dimensions of the analyzed models.

Butt joint plate	Dimensions	Units
t	12	mm
L	300	mm
W	50	mm
T-joint plate	**Dimensions**	**Units**
t	12	mm
H	163	mm
L	320	mm
W	50	mm

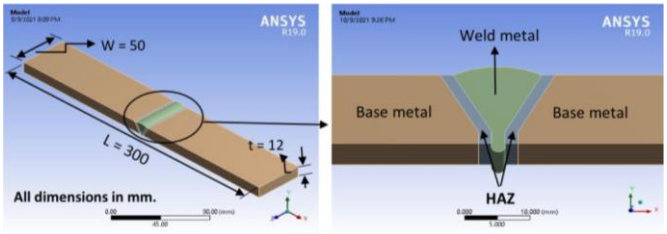

(a) geometry of butt joint. **(b)** cross-sectional view of weld joint.

Fig. 1 plate geometry design of butt joint.

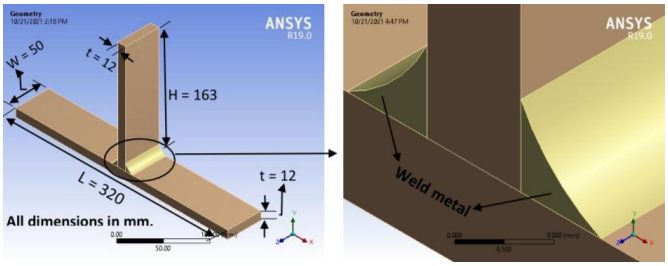

(a) T-joint fillet weld design. **(b)** cross-section of weld joint design.

Fig. 2 design of the T-joint fillet weld plate geometry.

2.3. Simulation of welding flaws

Linear misalignment flaw is the first case study that was expressed by a mismatch between two welded pieces such that while their surface planes are parallel, they are not in the required plane. Undercut flaw is the second case study that was indicated by a surface depression along the junction between the weld metal and parent metal and caused by excessive current and other factors during the welding process. Figure 3 shows studied welding defects above where, (*e*) is the value of the misalignment level, (*l*) is the undercut's length, (*v*) is the undercut's width and (*d*) is the depth of the undercut.

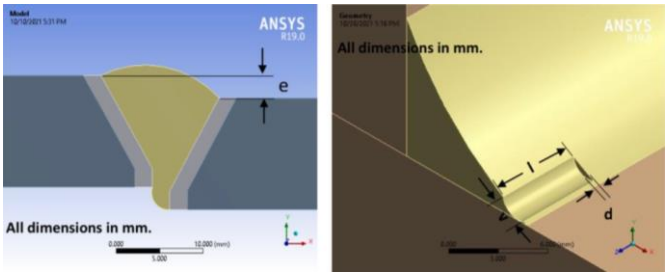

(a) misalignment defect. **(b)** undercut defect.

Fig. 3 simulation view of the studied welding defects.

2.4. Meshing

The elements were generated with automatic mesh for the base metal and patch conforming method, tetrahedrons mesh for the weld metal zones. The element size was 2 mm and refinement option were generated at the defect locations. The constructed models are revealed in Fig. 4.

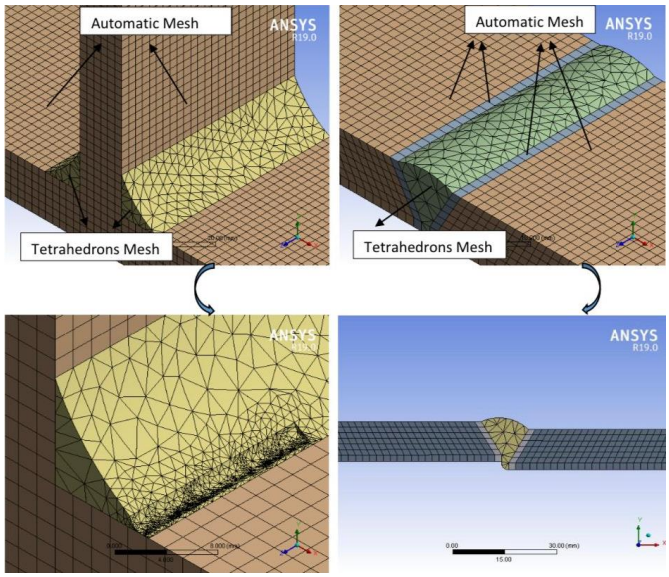

(a) undercut defect. **(b)** misalignment defect.

Fig. 4 Finite element meshing.

3. Results and discussion

3.1. Validation of finite element model

3.1.1. Validation without welding defects

The results of the FEM analysis using ANSYS Workbench Software were confirmed by comparing with Heshmati [9] for numerical analysis of longitudinal non-load carrying attachment using ABAQUS Tool. The comparison was good with error percentage 3 %. The findings of the FEM study were likewise compared to those of Steimbreger [10] for a transverse non-carrying load fillet joint experimental test. The comparison has been good with error percentage 4 %. Figures 5 and 6 show the validations above with Heshmati [9] and Steimbreger [10] respectively.

The percentage errors were calculated by the equation below and Table 3 illustrates these errors with clarification.

$$Error\ \% = \frac{|\ Ref. - FEM\ |}{Ref.} \times 100\ \% \qquad (1)$$

Table 3. The comparison between the present work of the FEM analysis with the Heshmati [9] and with the Steimbreger [10].

FEM analysis values (cycles)	Heshmati [9] values (cycles)	Percentage errors (%)	FEM analysis values (cycles)	Steimbreger [10] values (cycles)	Percentage errors (%)
10087	10288	1.96	1.03E+05	1.07e+5	3.98
20926	21180	1.2	1.25E+05	1.3E+05	3.9
30961	31235	0.88	1.74E+05	1.814E+05	4.1
45000	45180	0.4	2.69E+05	2.8066E+05	4.155
7.00E+04	70470	0.668	4.82E+05	5.02E+05	3.99
9.00E+04	91037	1.14	7.97E+05	8.296E+05	3.94
1.50E+05	155440	3.5	1.11E+06	1.157E+06	4.14
3.50E+05	378173	7.45	1.60E+06	1.671E+06	4.275
7.00E+05	774936	9.67	2.55E+06	2.66E+06	4.14
Average error		3 %	Average error		4 %

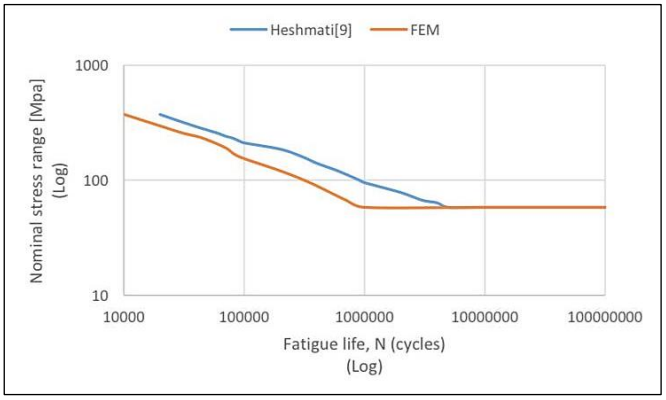

Fig. 4 validation with Heshmati [9] for numerical analysis without welding defects.

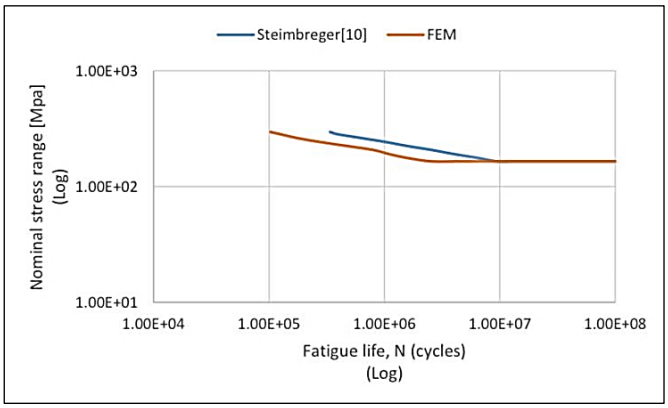

Fig. 5 validation with Steimbreger [10] for experimental test without welding defects.

The data of Figs. 4 and 5 for researchers Heshmati [9] and steimbreger [10] respectively were obtained by the program of Get Data Graph Digitizer version 2.24.

3.1.2. Validation with welding defects

FEM results were compared with Nguyen [8] for experimental tests of butt joint plates in case of welding defects such as linear misalignment with a wide range of defect levels; (*e*/*t*) where, (*e*) is the value of the misalignment level, (*t*) is the plate thickness, while (*e*/*t*) is the ratio of the misalignment level to the plate thickness. The validation done using nominal stress method and structural hot spot stress method. Both methods gave a good comparison with error percentage 2 %. Figure 6 shows the validation with Nguyen [8] using the two methods above.
Table 4 illustrates percentage errors with clarification.

Table 4. The comparison between the present work of the FEM analysis with the Nguyen [8].

FEM analysis values (cycles)	Nguyen [8] values (cycles)	Percentage errors (%)
2.84E+04	2.899E+04	2.04
6.56E+04	6.696E+04	2.025
1.51E+05	1.541E+05	2.055
2.30E+05	2.348E+05	2.0778
3.50E+05	3.572E+05	2.035
5.31E+05	5.424E+05	2.1156
1.23E+06	1.256E+06	2.1375
Average error = 2 %		

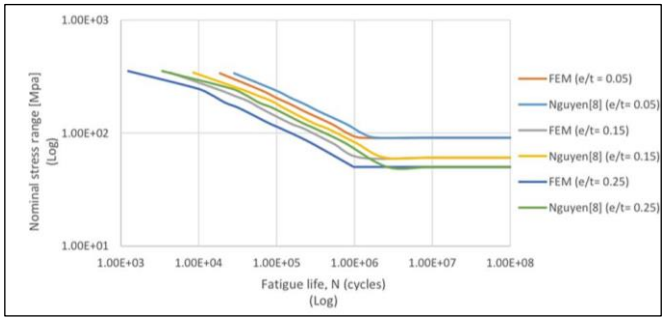

(a) validation with Nguyen [8] in accordance with the nominal stress method.

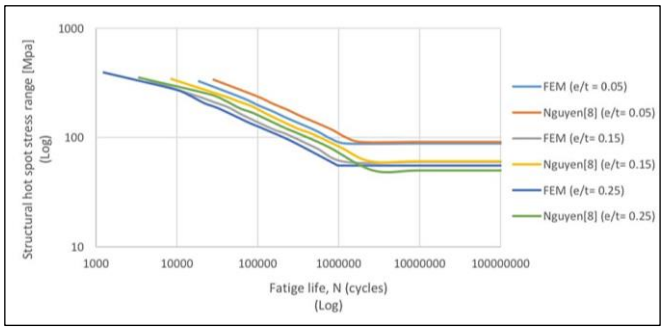

(b) validation with Nguyen [8] in accordance with the structural hot spot stress method.

Fig. 6 validation with Nguyen [8] for experimental test of butt joint with misalignment defect.

The data of Fig. 6 for researcher Nguyen [8] were obtained by the program of Get Data Graph Digitizer version 2.24.

3.2. Case Study No. 1: butt joint plate with misalignment defect

The input parameter is the value of the misalignment level (*e*) which is expressed as a proportion of plate thickness (*e/t*). Six ratios of misalignment levels (*e/t*) are considered which are 0.025, 0.05, 0.10, 0.15, 0.20 and 0.25 for this case. Figure 7 shows the contours of Maximum Principal Stress distribution for *e/t* = 0.20.

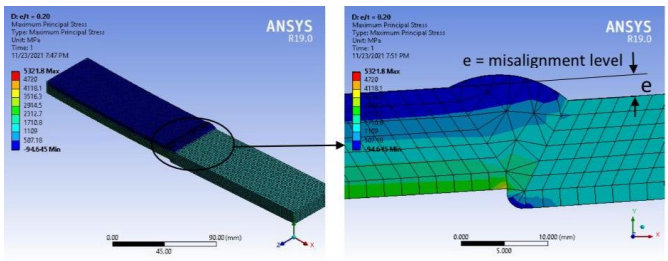

Fig. 7 Maximum Principal Stress distribution for e/t = 0.20.

The fatigue life (*N*) of butt joint is lowered by 10.8 % - 50.2 % when the flaw ratio (*e/t* = 0.025 - 0.25) as compared to aligned plate because with increased misalignment, the maximum principal stress rises accompanied by a reduction in fatigue life of the plate. Figure 8 shows impact of misalignment on fatigue life of butt joint.

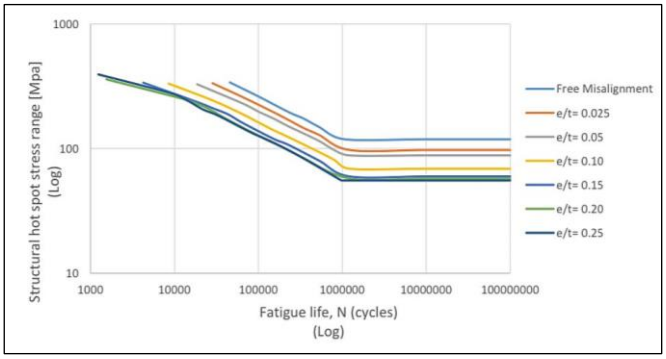

Fig. 8 Impact of misalignment defect on fatigue life (*N*) of butt joint.

By regression analysis for fatigue life of the misalignment defect, a nonlinear relationship between the fatigue life (*N*) and the misalignment level (*e/t*) produced and it shown in equation below.

$$N = 39438.317 - 42428.869(e/t) + 16574.711(e/t)^2 - 2227.643\,(e/t)^3 + 6809624.267(1/\sigma) \quad (2)$$

σ = Applied stress.

Equation (2) was deduced through a data fit program IBM SPSS Statistics 26.0.

Figure 9 shows comparison between the present results of finite element method for the misalignment defect and the obtained equation, i.e. eq. (2). It is clear that the equation gives a good agreement with acceptable error percentage 10.21 %. Table 5 illustrates the percentage errors with clarification.

Table 5. The comparison between the present work of the FEM analysis with the eq. (1).

FEM analysis values (cycles)	Regression analysis values (cycles)	Percentage errors (%)
28411.4	32179.635	11.71
65597.5	73240.105	10.435
1.51E+05	1.68E+05	10.135
2.30E+05	2.543E+05	9.585
3.50E+05	3.888E+05	9.985
5.31E+05	5.813E+05	8.66
1.23E+06	1.38E+06	10.985
Average error = 10.21 %		

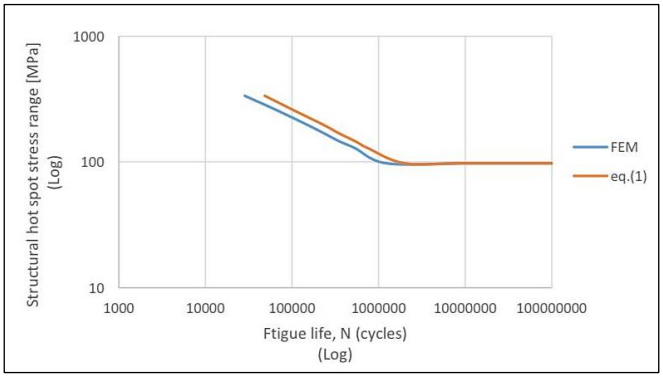

Fig. 9 Comparison between FEM results and eq. (1) for the misalignment defect.

3.2. Case Study No. 2: T-Joint plate with undercut flaw

The input parameters are undercut depth, undercut width and undercut length. In this case four ratios of flaw depth (d/t) are taken into account that are 0.0267, 0.043, 0.063, and 0.083 where (d) is the value of the defect depth and (t) is the plate thickness. Also, four defect width ratios (v/z) are considered which are 0.232, 0.348, 0.465 and 0.581 where (v) is the value of the defect width and (z) is the value of the weld leg. Also, four defect length ratios (l/w) are considered which are 0.12, 0.24, 0.36 and 0.48 where (l) is the value of the defect length and (w) is the plate width. Figure 10 illustrates the undercut defect's geometry and the contours of the Maximum Principal Stress distribution around it.

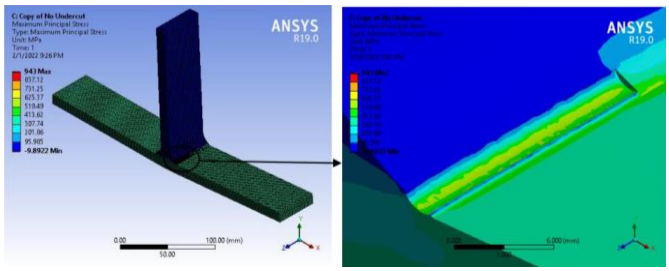

Fig. 10 Distribution of Maximum Principal Stress around the flow.

Most dangerous dimensions of this defect were d/t = 0.083, v/z = 0.232 and l/w = 0.36 because at these dimensions the maximum principal stress was the highest because of increase stress concentration at the weld toe zone and therefore result in decrease the fatigue life of the plate. Figure 11 shows influence of undercut on fatigue life of T-Joint at the most dangerous dimensions of the defect.

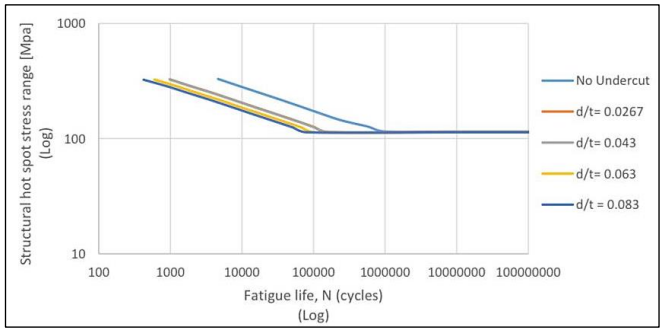

(a) Impact of undercut depth (d/t) on the fatigue life (N) of T-Joint (constant parameters: v/z = 0.232 and l/w = 0.36).

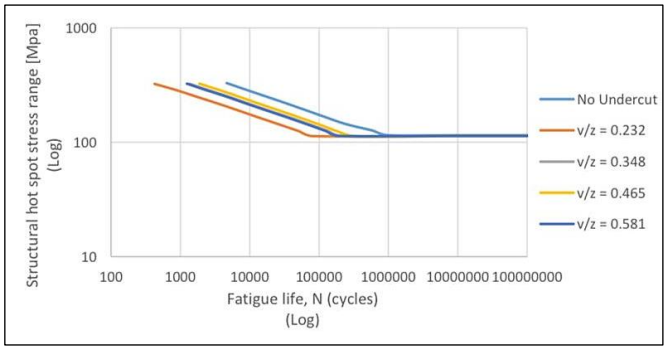

(b) Effect of undercut width (v/z) on the fatigue life (N) of T-Joint (constant parameters: d/t = 0.083 and l/w = 0.36).

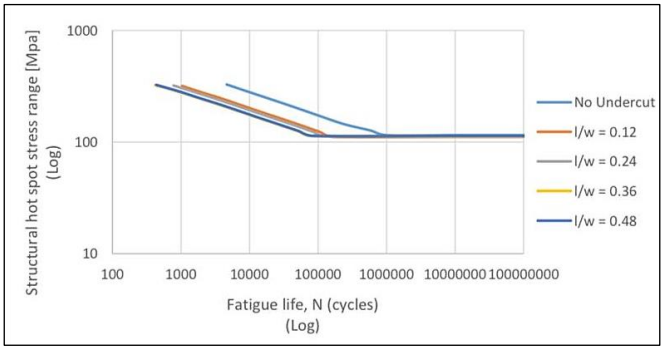

(c) Impact of undercut length (l/w) on the fatigue life (N) of T-Joint (constant parameters: d/t = 0.083 and v/z = 0.232).

Fig. 11 Impact of undercut defect on the fatigue life (N) of T-Joint.

By regression analysis for fatigue life of the undercut defect, a nonlinear relationship between fatigue life (N) and fatigue life variables d/t, v/z and l/w produced and it shown in equations below.

$$N = -476.519 + 9465.833(d/t) - 16490.076(d/t)^2 + 8072.636(d/t)^3 + 212099.214(1/\sigma) \quad (3)$$

$$N = 229.009 - 1044.005(v/z) + 841.98(v/z)^2 - 117.315(v/z)^3 + 90440.217(1/\sigma) \quad (4)$$

$$N = 897.407 + 119.665(1/w) - 14.076(1/w)^2 + 0.356(1/w)^3 + 219405.291(1/\sigma) \quad (5)$$

σ = applied stress

Equations (3)-(5) were deduced through a data fit program (IBM SPSS Statistics 26).

Figure 12 compares current results of finite element method for the undercut defect with the obtained equations, i.e. eqs. (3)-(5). It is clear that the equations give a good agreement with acceptable error percentages 0.55 % for defect depth, 1.73% and 0.45 % for defect width and defect length respectively.

Tables 6, 7, and 8 illustrate the percentage errors with clarification.

Table 6. the comparison between the present work of the FEM analysis with the eq. (3).

FEM analysis values (cycles)	Regression analysis values (cycles)	Percentage errors (%)
983.15	990.23	0.715
1865	1875.465	0.558
3653.3	3668.855	0.424
7409.7	7431.772	0.297
14845	14889.22	0.297
25789	25909.479	0.465
56375	56576.412	0.356
1.03E+05	103475.989	0.46
1.57E+05	159156.571	1.355
Average error = 0.55 %		

Table 7. the comparison between the present work of the FEM analysis with the eq. (4).

FEM analysis values (cycles)	Regression analysis values (cycles)	Percentage errors (%)
423.29	430.185	1.603
893.96	907.693	1.513
1714.1	1741.688	1.584
3621.8	3676.618	1.491
7350.9	7460.191	1.465
12565	12784.64	1.718
27691	28132.111	1.568
51758	52638.644	1.673
80979	83431.897	2.94
Average error = 1.73 %		

Table 8. the comparison between the present work of the FEM analysis with the eq. (5).

FEM analysis values (cycles)	Regression analysis values (cycles)	Percentage errors (%)
1043.1	1047.026	0.375
1968	1975.923	0.401
3869.3	3885.19	0.409
7811.1	7842.784	0.404
15681	15744.45	0.403
27278	27404.333	0.461
59461	59715.387	0.426
1.08E+05	108504.546	0.465
1.65E+05	166174.8562	0.707
Average error = 0.45 %		

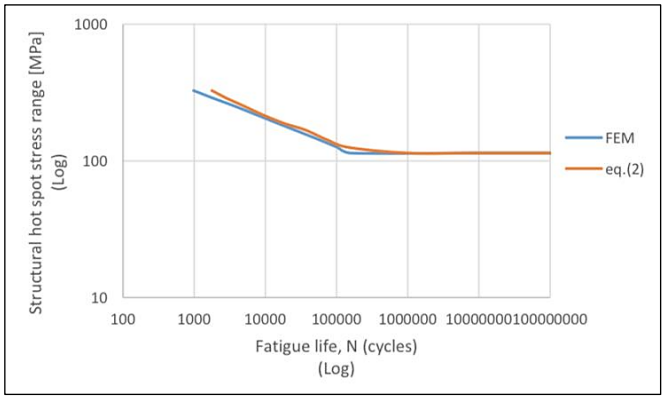

(a) Comparison between FEM results and eq. (3) for the undercut depth (d/t).

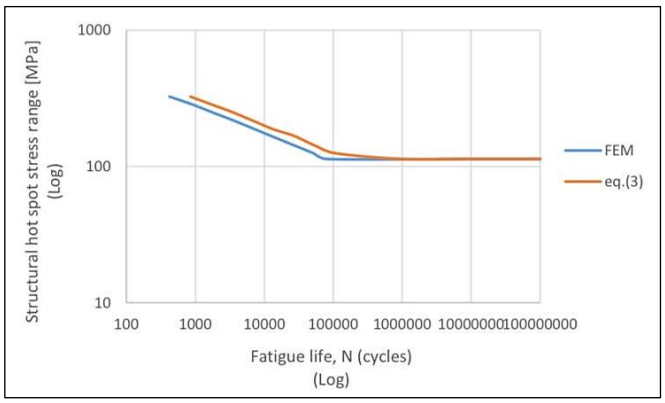

(b) Comparison between FEM results and eq. (4) for the undercut depth (v/z)

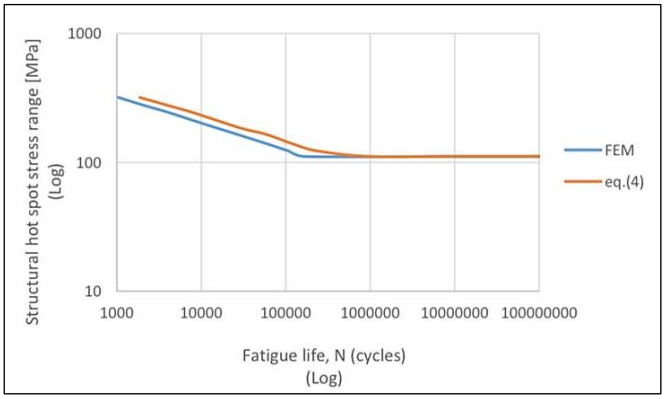

(c) Comparison between FEM results and eq. (5) for the undercut depth ($1/w$).

Fig. 12 Comparison between FEM results and eqs. (3)-(5) for the undercut defect.

3.3. Case Study No. 3: T-Joint plate with porosity defect

The input variables for T-joint plate with porosity defect are porosity diameter, porosity number and porosity location. For this case three defect diameters (d) are considered which are 1.0 mm, 1.5 mm and 2.0 mm. Also, six defect numbers (n) and four defect locations are considered. Figure 14 illustrates the porosity flaw's geometry and contours of the Maximum Principal Stress distribution around it.

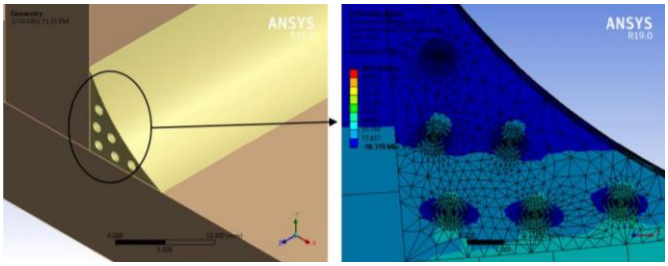

Fig. 13 Maximum Principal Stress distribution around the flaw.

Most dangerous variables of porosity defect were d = 2.0 mm and n = 6 because the weld metal zone becomes weak as the numbers of porosity increased, especially when it is 2 mm (maximum diameter). Figure 14 shows effect of porosity on fatigue life of T-joint at the most dangerous variables of the defect.

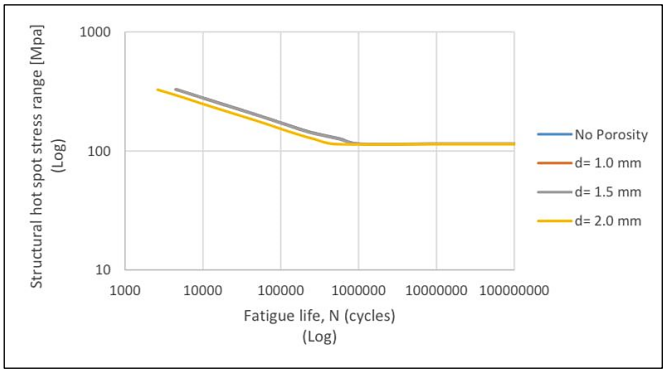

(a) Effect of flow diameter (d) on fatigue life (N) of T-Joint (constant parameter: n = 6).

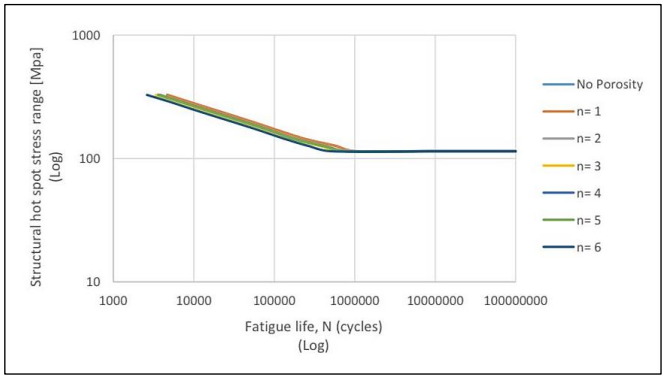

(b) Effect of flow number (*n*) on fatigue life (*N*) of T-Joint (constant parameter: *d* = 2 mm).

Fig. 14 Effect of the porosity defect on fatigue life (*N*) of T-Joint.

By regression analysis for fatigue life of porosity defect, a nonlinear relationship between fatigue life (*N*) and fatigue life variables (*d*) and (*n*) produced and it shown in equations below.

$$N = 6851.616 + 8389.1(d) - 3431.8(d)^2 - 3346.32(n) + 989.296(n)^2 - 92.683(n)^3 + 1012139.843(1/\sigma) \quad (6)$$

σ = applied stress.

Equation (6) was deduced through a data fit program (IBM SPSS Statistics 26).

Figure 15 shows comparison between the present results of finite element method for the porosity defect and the obtained equation, i.e. eq. (5). It is clear that the equation gives a good agreement with acceptable error percentages 5.14 % and 1.65 % for the defect diameter and defect numbers respectively. Tables 9 and 10 illustrate these errors with clarification.

Table 9. the comparison between the present work of the FEM analysis with the eq. (6).

FEM analysis values (cycles)	Regression analysis values (cycles)	Percentage errors (%)
4532.2	4765.018	4.886
8394.2	8840.466	5.048
15630	16484.038	5.181
31891	33621.144	5.146
63958	67423.571	5.14
1.08E+05	114207.16	5.435
2.33E+05	246060.913	5.308
5.62E+05	591305.08	4.956
1.00E+06	1054652.07	5.182
Average error = 5.14 %		

Table 10. the comparison between the present work of the FEM analysis with the eq. (6).

FEM analysis values (cycles)	Regression analysis values (cycles)	Percentage errors (%)
4643	4739.883	2.044
8585	8713.436	1.474
16002	16263.682	1.609
32666	33187.036	1.57
65460	66502.087	1.567
1.10E+05	112093.914	1.868
2.41E+05	245207.765	1.716
5.81E+05	589010.543	1.36
1.00E+06	1016694.117	1.647
Average error = 1.65 %		

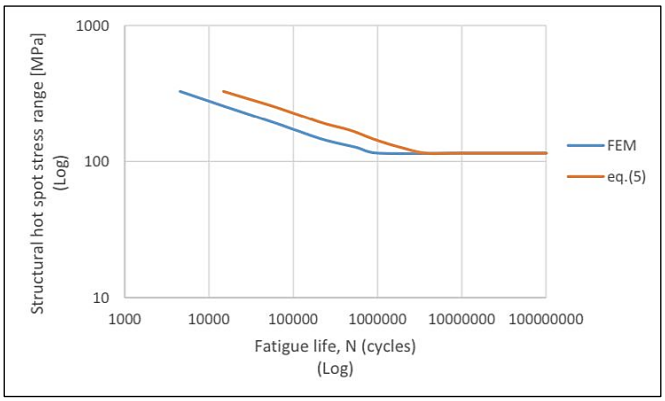

(a) comparison between FEM results and eq. (6) for the porosity diameter (d)

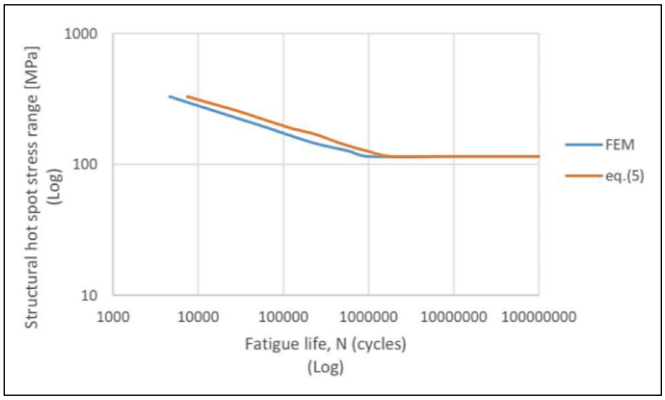

(b) comparison between FEM results and eq. (6) for the porosity numbers (n)

Fig. 15 comparison between FEM results and eq. (6) for the porosity defect.

Additional case was considered which is porosity location (for *d* = 1.0 mm). Four defect locations are considered as shown in figure below. The most dangerous location is fourth location because porosity is near to the weld toe area and it is a stress concentration zone. Figs. 16 and 17 show effect of flaw location on fatigue life of T-joint.

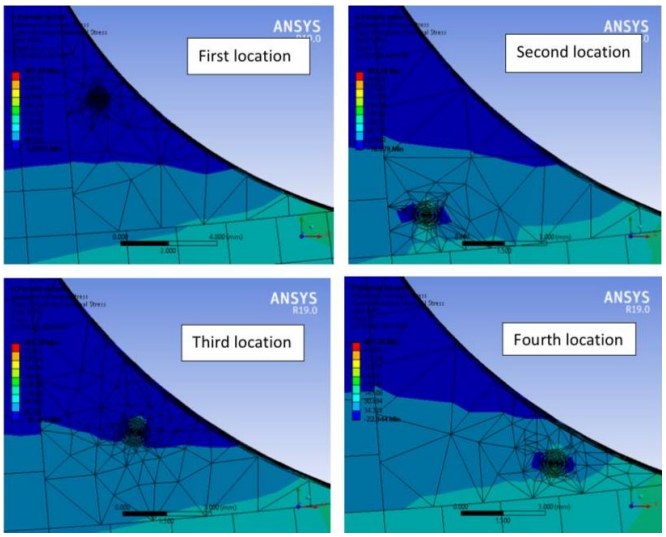

Fig. 16 Maximum Principal Stress distribution around porosity at different locations.

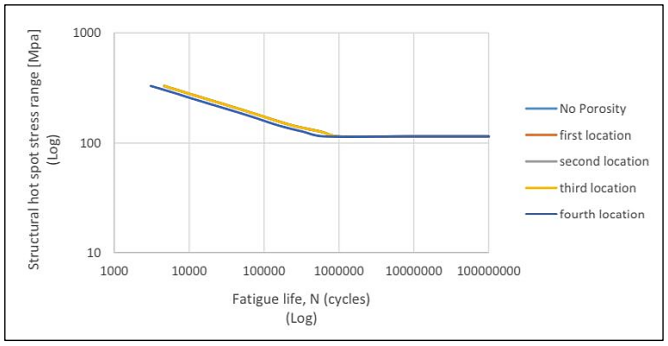

Fig. 17 Effect of flow location on the fatigue life (N) of T-joint at different locations when d = 1.0 mm.

4. Conclusions

Fatigue life (N) estimated using FEM with three forms of welding flaws in this study that are misalignment defect for butt joint plate, undercut and porosity defects for T-joint plate with various dimensions for each defect. The following findings concluded as a result of this research.

1. There was a strong agreement between finite element simulation with the previously published experimental fatigue life assessments, with the comparison revealing a more accurate estimation with a maximum error of 4 %.
2. With rising levels of misalignment, fatigue life (N) and fatigue limit of butt joint were reduced. while the fatigue life (N) of T-joint is decreased with increasing levels of undercut and porosities without decreasing its fatigue limit.
3. The undercut defect is more dangerous than the porosity defect for T-joint plate. As a result, it's necessary to find the flaw before service starts.
4. For the undercut defect, the defect width affects the fatigue life (N) of T-joint more than its length and depth. And for the porosity defect, the effect of the diameter was almost the same as the number of porosities on the fatigue life (N).

References

[1] D. Deng, W. Liang, and H. Murakawa, "Determination of welding deformation in fillet-welded joint by means of numerical simulation and comparison with experimental measurements", Journal of Materials Processing Technology, Vol. 183, Issue 2-3, pp. 219-225, 2007. https://doi.org/10.1016/j.jmatprotec.2006.10.013

[2] F. R. Mashiri, X. L. Zhao, and P. Grundy, "Effect of weld profile and undercut on fatigue crack propagation life of thin-walled cruciform joint", Thin-Walled Structures, Vol. 39, Issue 3, pp. 261-285, 2001. https://doi.org/10.1016/S0263-8231(00)00061-6

[3] J. Frostevarg, and A. F. H. Kaplan, "Undercuts in Laser Arc Hybrid welding", Physics Procedia, Vol. 56, pp. 663-672, 2014. https://doi.org/10.1016/j.phpro.2014.08.071

[4] C. Steimbreger and M. D. Chapetti, "Fracture mechanics based prediction of undercut tolerances in industry", Engineering Fracture Mechanics, Vol. 211, pp. 32-46, 2019. https://doi.org/10.1016/j.engfracmech.2019.02.006

[5] R. M. Andrews, "The Effect of Misalignment on the Fatigue Strength of Welded Cruciform Joints", Fatigue and Fracture of Engineering Materials and Structures, Vol. 19, pp. 755-768, 1996. https://doi.org/10.1111/j.1460-2695.1996.tb01320.x

[6] M. J. Ottersböck, M. Leitner, M. Stoschka, and W. Maurer, "Analysis of fatigue notch effect due to axial misalignment for ultra high-strength steel butt joints", Welding in the World, Vol. 63, pp. 851-865, 2019. https://doi.org/10.1007/s40194-019-00713-4

[7] E. Surojo, J. Anindito, F. Paundra, A. R. Prabowo, E. P. Budiana, N. Muhayat, M. Badaruddin, and Triyono, "Effect of water flow and depth on fatigue crack growth rate of underwater wet welded low carbon steel SS400", Open Engineering, Vol. 11, Issue 1, pp. 329-338, 2021. https://doi.org/10.1515/eng-2021-0036

[8] N. T. Nguyen, and M. A. Wahab, "The Effect of Undercut and Residual Stresses on Fatigue Behavior of Misaligned Butt Joints", Engineering Fracture Mechanics, Vol. 55, Issue 3, pp. 453-469, 1996. https://doi.org/10.1016/0013-7944(96)00024-0

[9] M. Heshmati, "Fatigue Life Assessment of Bridge Details Using Finite Element Analysis", M.Sc. thesis, Department of Civil and Environmental Engineering, Chalmers University of Technology, Sweden, 2012.

[10] C. Steimbreger, "Fatigue of Welded Structures", M.Sc. thesis, Deparment of Engineering Sciences and Mathematics, Lulea University of Technology, Sweden, 2014.

[11] N. A. Saleh, R. J. Jasim, and H. S. Jasim, "Failure Pressure Predicted in Oil Pipe Lines with Welding Defects", IOP Conference Series: Materials Science and Engineering, Vol. 745, 2020. https://doi.org/10.1088/1757-899X/745/1/012057